A transport equation model that is consistent with Monte Carlo simulations of ion implantation into infinite targets

A transport equation model that is consistent with Monte Carlo simulations of ion implantation into infinite targets

R Oven, M D J Bowyer and D G Ashworth

Solid State Electronics Group, Electronic Engineering Laboratories, University of Kent, Canterbury CT2 7NT, UK

Abstract. In this paper a transport equation (TE) is derived that matches closely (within the limitation of an infinite target) the transport model in the Monte Carlo code TRIM. Initially, we derive a TE that incorporates an arbitrary free-flight path length distribution function and a stopping energy. From this TE a coupled set of integral equations (for spatial moments up to order four) incorporating the *liquid* free-flight path model used in TRIM is derived. These integral equations for the liquid model are incorporated into a revised version of the transport theory computer code KUBBIC using the two-parameter differential nuclear scattering cross section. Also, for the *gas-like* model of the free-flight path length distribution, the equivalence is shown between the new TE and the LSS backward linearized Boltzmann equation extended by Brice to include an intermediate energy. A comparison between gas-like and liquid models is performed for the ion As implanted into aSi using both the KUBBIC code and a parallel processor MC code based on TRIM. Excellent agreement is obtained between the computer codes, even at very low energies, *when using the same free-flight path models and stopping energies*. Significant deviations occur, however, between the gas-like and liquid models at energies below $\sim 10\,\text{keV}$, when both models are used in the same code.

1. Introduction

In a previous paper (Bowyer *et al* (1992a), hereinafter referred to as I) we performed high-resolution comparisons of the first eight moments of the range distribution of ions implanted into an amorphous homogeneous target as derived from two computer codes. The codes in question were a high-speed parallel processor Monte Carlo (MC) computer code based on TRIM (Ziegler *et al* 1985), and our newly developed transport theory code KUBBIC employing an iterative solution technique (Winterbon 1986). To facilitate direct comparison, effort was made to match input quantities. Specifically, both codes incorporate nuclear scattering using the *universal* interatomic potential and Biersack's two-parameter *magic* formula (Ziegler *et al* 1985, ch 2) and the electronic energy-loss formalism described in Ziegler *et al* (1985) ch 3. To match assumptions inherent in KUBBIC, the MC code was modified to treat targets of infinite extent and to use the *gas-like* model (in which the distribution of the free-flight path length is described by Poisson statistics (see, for example, Eckstein (1991) ch 7)) in place of the *liquid* model (in which a δ function describes the free-flight path length distribution (Miyagawa and Miyagawa 1983; Eckstein 1991)) used in TRIM. Good agreement was obtained between KUBBIC and the modified MC code. However, when KUBBIC was compared with the MC code using the liquid model, poor agreement was apparent

at energies below ~ 30 keV for As ions implanted into aSi. The inadequacy of the one-parameter differential nuclear scattering cross section to predict third- and fourth-order moments was also demonstrated. Our aim in this paper is to derive a transport model that matches as closely as possible the MC code TRIM (still within the limitations of an infinite target). In order to perform this we first derive a transport equation (TE) incorporating an arbitrary free-flight path length distribution function. The new TE includes explicitly the electronic energy loss as a frictional force integrated over the free-flight path, and a minimum energy at which the ion is assumed to stop. We show how this TE can be evaluated for both gas-like and liquid models. The TE using the liquid model has been implemented in a revised version of KUBBIC. Excellent agreement is obtained between KUBBIC incorporating the liquid model and the MC code incorporating the liquid model (as is the agreement between KUBBIC and MC codes incorporating the gas-like model).

2. Derivation of the TE using an arbitrary free-flight path length distribution function

We wish to calculate the ion rest distribution function for an ion implanted into an amorphous homogeneous target of infinite extent, which is characterized by a free-flight path length distribution function $f(l)$. We define $F(E, \hat{u}, E_s, r)\mathrm{d}r$ as the probability that an ion, of initial energy E and velocity direction given by the unit vector $\hat{u}$, comes to rest (i.e. reaches an energy E_s) at a vector range between r and $r + \mathrm{d}r$. The function $F(E, \hat{u}, E_s, r)$ is normalized such that

$$\int_r F(E, \hat{u}, E_s, r)\mathrm{d}r = 1 \tag{1}$$

where the integration is performed over all r. If E is less than E_s then the ion does not travel any distance, hence

$$F(E, \hat{u}, E_s, r) = \delta(r) \qquad \text{for} \quad E < E_s. \tag{2}$$

The free-flight path length distribution $f(l)$ is defined such that $f(l)\mathrm{d}l$ is the probability that an ion will travel a distance between l and $l + \mathrm{d}l$, between binary collisions, and is normalized such that

$$\int_0^\infty f(l)\mathrm{d}l = 1. \tag{3}$$

Consider the ion starting from the origin with initial energy E and velocity direction $\hat{u}$ (see figure 1). It will travel in the direction $\hat{u}$ until it undergoes its first collision. Assuming that the interaction of the ion with the electronic structure can be represented as a frictional force, then to travel a distance l the ion will lose an energy T_l given by

$$T_l = N \int_0^l S_e(E)\mathrm{d}l \tag{4}$$

where $S_e(E)$ is the electronic stopping power and N is the target atomic density. The collision at l will result in the ion changing state from $[E - T_l, \hat{u}]$ to $[E - T_l - T_n, \hat{u}']$,
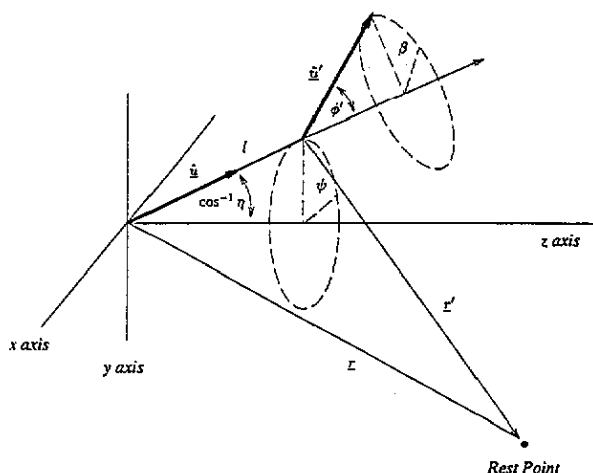
Figure 1. Geometry associated with the scattering event.

where T_n is the energy transferred to the target atom during the collision and $\hat{u}'$ is the direction of motion of the scattered ion. Assuming binary elastic collisions the probability of the ion changing state may be written as (Winterbon *et al* 1970)

$$\frac{\mathrm{d}\sigma_n(E - T_l, T_n, \hat{u}, \hat{u}')}{\sigma_n} = \frac{\mathrm{d}\sigma_n(E - T_l, T_n)}{\sigma_n}\delta(\hat{u}\cdot\hat{u}' - \cos\phi'(E - T_l, T_n))\frac{\mathrm{d}\beta}{2\pi}$$

$$\equiv \frac{\mathrm{d}\tilde{\sigma}_n}{\sigma_n}\frac{\mathrm{d}\beta}{2\pi} \tag{5}$$

where $\mathrm{d}\sigma_n$ is the differential nuclear scattering cross section, ϕ' is the scattering angle in the laboratory system, β is the azimuthal scattering angle and σ_n is the total nuclear scattering cross section. The probability that an ion travels a distance between l and $l + \mathrm{d}l$ whilst continuously slowing down to reach a state $[E - T_l, \hat{u}]$, and then gets scattered into a state $[E - T_l - T_n, \hat{u}']$, is given by

$$f(l)\mathrm{d}l\frac{\mathrm{d}\tilde{\sigma}_n}{\sigma_n}\frac{\mathrm{d}\beta}{2\pi}. \tag{6}$$

If the ion undergoes a scattering event then it has a probability density $F(E - T_l - T_n, \hat{u}', E_s, r')$ of coming to rest at r, where, from figure 1, $r' = r - \hat{u}l$. Hence, the probability density that the ion travels a free-flight path length between l and $l + \mathrm{d}l$, gets scattered into state $[E - T_l - T_n, \hat{u}']$, and eventually comes to rest at r, is

$$f(l)\mathrm{d}lF(E', \hat{u}', E_s, r - \hat{u}l)\theta(E' - E_s)\frac{\mathrm{d}\tilde{\sigma}_n}{\sigma_n}\frac{\mathrm{d}\beta}{2\pi} \tag{7}$$

where $E' = E - T_l - T_n$. There is zero probability of this occurring if E' falls below E_s. This is represented by a unit step function $\theta(\cdot)$. Summing (7) over all possible path lengths and states gives the probability density that the ion will scatter and come to rest at r:

$$\int_0^\infty f(l)\left(\int_0^{2\pi}\int_{T_{\min}}^{T_{\max}} F(E', \hat{u}', E_s, r - \hat{u}l)\theta(E' - E_s)\frac{\mathrm{d}\tilde{\sigma}_n}{\sigma_n}\frac{\mathrm{d}\beta}{2\pi}\right)\mathrm{d}l \tag{8}$$

where T_{max} and T_{min} are the maximum and minimum energies transferred in a binary collision and we have assumed $f(l)$ to be energy independent. The unit step function $\theta(\cdot)$ limits the range of integration to scattering events that give $E' > E_s$. If either the electronic energy loss or the scattering event causes E' to fall below E_s then the ion has stopped at $r = \hat{u}l$. The probability that the ion does not travel further because it has energy less than E_s is given by

$$\int_{T_{min}}^{T_{max}} \theta(E_s - E') \frac{d\bar{\sigma}_n}{\sigma_n}. \tag{9}$$

Hence the probability density of ions stopped after the first collision is

$$\int_0^\infty f(l) \left(\int_{T_{min}}^{T_{max}} \theta(E_s - E') \frac{d\bar{\sigma}_n}{\sigma_n} \right) \delta(r - \hat{u}l) \, dl. \tag{10}$$

The sum of the probability densities in (8) and (10) gives the original probability density:

$$F(E, \hat{u}, E_s, r) = \int_0^\infty f(l) \left(\int_0^{2\pi} \int_{T_{min}}^{T_{max}} F(E', \hat{u}', E_s, r - \hat{u}l) \theta(E' - E_s) \frac{d\bar{\sigma}_n}{\sigma_n} \frac{d\beta}{2\pi} \right) dl$$

$$+ \int_0^\infty f(l) \left(\int_{T_{min}}^{T_{max}} \theta(E_s - E') \frac{d\bar{\sigma}_n}{\sigma_n} \right) \delta(r - \hat{u}l) \, dl. \tag{11}$$

This is an integral equation governing the probability density function. A number of functions can be used for $f(l)$. In addition to the gas-like and liquid models mentioned so far, a more realistic function can, in principle, be obtained by computer simulation using the amorphous target mode of the crystalline-target binary collision code MARLOWE (Robinson and Torrens 1974, Eckstein 1991). Using the gas-like model we have shown the equivalence between (11) and a vector version (Littmark and Gras-Marti 1978) of the LSS backward-linearized Boltzmann equation (Lindhard *et al* 1963) extended by Brice (1971) to include an intermediate energy. An outline of this derivation is shown in the appendix. Biersack (1982) has presented a TE for the liquid model and has given qualitative assessments concerning the mean projected range and vertical straggling. However, no attempt was made to develop a full moment solution and a stopping energy was not considered.

3. Moments solution for a plane-source TE

In this section we take moments of a plane-source TE and then expand using Legendre polynomials in order to obtain a general set of coefficients from which vertical, lateral and mixed moments can be obtained. A set of eight such coefficients can provide moments up to order four.

To simplify development, we define $F(E, \eta, E_s, z) \, dz$ as the probability that an ion of initial energy E comes to rest (i.e. reaches an energy E_s) at a depth between z and $z + dz$ when the ion starts in the direction $\cos^{-1} \eta$ with respect to the z axis. This distribution is normalized such that

$$\int_{-\infty}^\infty F(E, \eta, E_s, z) \, dz = 1. \tag{12}$$

The point-source density function $F(E, \hat{u}, E_s, r)$, using the angle ψ as defined in figure 1, can be written as $F(E, \eta, \psi, E_s, x, y, z)$. The plane-source density function is related to the point-source density function by

$$F(E, \eta, E_s, z) = \frac{1}{2\pi} \int_0^{2\pi} \int_{-\infty}^{\infty} \int_{-\infty}^{\infty} F(E, \eta, \psi, E_s, x, y, z) \, dx \, dy \, d\psi. \tag{13}$$

Performing the integrations in equation (13) on both sides of equation (11) and using the fact that

$$\frac{1}{2\pi} \int_0^{\infty} \int_0^{2\pi} \int_{-\infty}^{\infty} \int_{-\infty}^{\infty} g(l) \delta(r - \hat{u}l) dx \, dy \, d\psi \, dl = \int_0^{\infty} g(l) \delta(z - \eta l) dl \tag{14}$$

where $g(l)$ is an arbitrary function of l, gives a TE for the plane-source density function:

$$F(E, \eta, E_s, z) = \int_0^{\infty} f(l) \left(\int_0^{2\pi} \int_{T_{\min}}^{T_{\max}} F(E', \eta', E_s, z - \eta l) \theta(E' - E_s) \right.$$
$$\left. \times \frac{d\sigma_n(E_l, T_n)}{\sigma_n} \frac{d\beta}{2\pi} \right) dl$$
$$+ \int_0^{\infty} f(l) \left(\int_{T_{\min}}^{T_{\max}} \theta(E_s - E') \frac{d\sigma_n(E_l, T_n)}{\sigma_n} \right) \delta(z - \eta l) dl \tag{15}$$

where

$$E_l = E - T_l \tag{16}$$

$$\eta' = \eta \cos \phi'(E_l, T_n) + \sqrt{1 - \eta^2} \sin \phi'(E_l, T_n) \cos \beta. \tag{17}$$

Assuming standard practice (Winterbon *et al* 1970), the dependence on depth can be removed by taking spatial moments of equation (15) and the dependence on the velocity direction can be decoupled by expanding in terms of Legendre polynomials $P_k(\eta)$ such that

$$F^n(E, \eta, E_s) = \int_{-\infty}^{\infty} F(E, \eta, E_s, z) z^n \, dz$$
$$\equiv \sum_{k=0}^{n} (2k + 1) F_k^n(E, E_s) P_k(\eta). \tag{18}$$

Next, we let $z_1 = z - \eta l$, followed by a binomial expansion of $(z_1 + \eta l)^n$. Integration over the azimuthal angle can be carried out by utilizing the addition theorem for Legendre polynomials. Then, multiplying each term of the resulting equation by $P_m(\eta)$ and integrating over all η, one obtains an equation governing the coefficients $F_m^n(E, E_s)$:

$$F_m^n(E, E_s) = \frac{1}{2} \int_0^{\infty} f(l) \sum_{s=0}^{n} {}^nC_s l^{n-s} \sum_{k=0}^{s} (2k + 1) \int_{-1}^{1} \eta^{n-s} P_m(\eta) P_k(\eta) d\eta$$
$$\times \int_{T_{\min}}^{T_{\max}} F_k^s(E', E_s) P_k(\cos \phi'(E_l, T_n)) \theta(E' - E_s) \frac{d\sigma_n(E_l, T_n)}{\sigma_n} \, dl$$
$$+ \frac{1}{2} \int_{-1}^{1} \eta^n P_m(\eta) d\eta \int_0^{\infty} f(l) l^n \left(\int_{T_{\min}}^{T_{\max}} \theta(E_s - E') \frac{d\sigma_n(E_l, T_n)}{\sigma_n} \right) dl. \tag{19}$$

Extracting the term $s = n$ from the first summation of (19), moving it to the LHS and introducing $r = n - s$, results in the equation

$$\int_0^\infty f(l) \int_{T_{\text{min}}}^{T_{\text{max}}} [F_m^n(E, E_s) - F_m^n(E', E_s) P_m(\cos \phi'(E_l, T_n)) \theta(E' - E_s)]$$

$$\times \frac{d\sigma_n(E_l, T_n)}{\sigma_n} dl$$

$$= \frac{1}{2} \int_0^\infty f(l) \sum_{r=1}^{n-1} {}^n C_r l^r \sum_{k=0}^{n-r} (2k+1) \int_{-1}^1 \eta^r P_m(\eta) P_k(\eta) d\eta$$

$$\times \int_{T_{\text{min}}}^{T_{\text{max}}} F_k^{n-r}(E', E_s) P_k(\cos \phi'(E_l, T_n)) \theta(E' - E_s) \frac{d\sigma_n(E_l, T_n)}{\sigma_n} dl$$

$$+ \frac{1}{2} \int_{-1}^1 \eta^n P_m(\eta) d\eta \int_0^\infty f(l) l^n dl. \tag{20}$$

An integral driver term of the form derived by Winterbon *et al* (1970) can be seen embedded in the LHS of (20), and on the RHS is a source term depending on coefficients of maximum order F_m^{n-1}. The form of this equation is important for two reasons. Firstly, the system of integral equations constructed has the property that the coupling between equations is one way, i.e. equations in the set for higher-order moments depend only on equations for lower-order moments. Secondly, for a numerical solution the integral driver can be approximated by a first-order ODE and used within an iterative solution scheme (Winterbon 1986).

4. Integral equations using the liquid model

So far the derivation has retained the arbitrary free-flight path distribution function $f(l)$. Introducing $f(l) = \delta(l - \lambda)$, where λ is the distance between nuclear events, a generator equation for the liquid model can be obtained:

$$N \int_{T_{\text{min}}}^{T_{\text{max}}} [F_m^n(E, E_s) - F_m^n(E', E_s) P_m(\cos \phi'(E_l, T_n)) \theta(E' - E_s)] d\sigma_n(E_l, T_n)$$

$$= \tfrac{1}{2} \lambda^{n-1} \int_{-1}^1 \eta^n P_m(\eta) d\eta + \tfrac{1}{2} \sum_{r=1}^{n-1} {}^n C_r \lambda^r \sum_{k=0}^{n-r} (2k+1)$$

$$\times \int_{-1}^1 \eta^r P_m(\eta) P_k(\eta) d\eta N \int_{T_{\text{min}}}^{T_{\text{max}}} F_k^{n-r}(E', E_s) P_k(\cos \phi'(E_l, T_n))$$

$$\times \theta(E' - E_s) d\sigma_n(E_l, T_n) \tag{21}$$

where $N = 1/\sigma_n \lambda$, and we have redefined E_l and E' as follows:

$$E_l = E - N S_e(E) \lambda \qquad E' = E - N S_e(E) \lambda - T_n. \tag{22}$$

These new definitions assume that the electronic stopping power remains constant over the path length λ. This approximation is used in TRIM versions 85 and 91.

5. Integral equations using the gas-like model

For the gas-like model we have

$$f(l) = (1/\lambda) \exp(-l/\lambda) \tag{23}$$

where λ is the mean distance between collisions. Inserting (23) into (11), and following arguments in the appendix, it can be shown that

$$N \int_{T_{\text{min}}}^{T_{\text{max}}} [F_m^n(E, E_s) - F_m^n(E - T_n, E_s) P_m(\cos \phi'(E, T_n))\theta(E - T_n - E_s)$$

$$- \theta(E_s - E + T_n)\delta_{n0}]\mathrm{d}\sigma_n(E, T_n) + N S_e(E)\frac{\mathrm{d}F_m^n(E, E_s)}{\mathrm{d}E}$$

$$= \frac{n[(m + 1)F_{m+1}^{n-1}(E, E_s) + m F_{m-1}^{n-1}(E, E_s)]}{2m + 1} \tag{24}$$

where δ_{n0} is a Kronecker delta. The normalization and initial conditions on F imply $F_0^0(E, E_s) = 1$. Using the gas-like model results in the normal separation of the electronic energy loss from the integral driver term. Equation (24) has been derived previously by Littmark and Gras-Marti (1978).

6. Implementation

Equation (21) can be rewritten using the notation

$$\mathcal{L}_m F_m^n(E, E_s) = S_m^n(E, E_s) \tag{25}$$

where the driver term in operator notation, $\mathcal{L}_m F_m^n(E, E_s)$, is given by the LHS of equation (21) and the source term $S_m^n(E, E_s)$ is given by the RHS of equation (21). Manipulation of (25) can be simplified by the substitution of the scattering integrals (appearing in the driver and source terms) by a new variable

$$\hat{F}_m^n(E', E_s) = N \int_{T_{\text{min}}}^{T_{\text{max}}} F_m^n(E', E_s) P_m(\cos \phi'(E_l, T_n))\theta(E' - E_s)\mathrm{d}\sigma_n(E_l, T_n). \tag{26}$$

The source coefficients $S_m^n(E, E_s)$ up to a given order can be computed in terms of the new variable resulting in a sum of products of $\hat{F}_k^{n-r}$ and powers of λ. The terms $\hat{F}_k^{n-r}$ can be back-substituted using

$$\hat{F}_m^n(E', E_s) = \lambda^{-1} F_m^n(E, E_s) - S_m^n(E, E_s). \tag{27}$$

The source terms required for the computation of moments up to a given order can be constructed using a symbolic algebra computer package. The integral

$$\hat{P}(r, m, k) = \int_{-1}^{1} \eta^r P_m(\eta) P_k(\eta)\mathrm{d}\eta \tag{28}$$

in equation (21) can be evaluated using the recurrence formula

$$\hat{P}(r,m,k) = \begin{cases} [2/(2m+1)]\delta_{mk} & r = 0 \\ \dfrac{(m+1)\hat{P}(r-1,m+1,k) + m\hat{P}(r-1,m-1,k)}{2m+1} & r > 0. \end{cases}$$

(29)

The source coefficients $S_m^n(E, E_s)$ required for moments up to order four are presented in table 1. In this table, for convenience, we have introduced the mean projected range $R_p = 3F_1^1$ and omitted the energy dependence on the coefficients $F_m^n(E, E_s)$. Comparing equations for the liquid model with the gas-like model reveals that the coefficients for the latter can be obtained from table 1 by setting $\lambda = 0$. In the light of (29) this is not surprising, since the form of the source coefficients for the gas-like model can be obtained by extracting the term $r = 1$ from the outer summation of (21).

Table 1. Liquid-model source coefficients S_m^n for moments up to order four.

$$S_1^1 = \tfrac{1}{3}$$
$$S_0^2 = -\tfrac{1}{3}\lambda + \tfrac{2}{3}R_p$$
$$S_2^2 = -\tfrac{2}{15}\lambda + \tfrac{4}{15}R_p$$
$$S_1^3 = \tfrac{1}{3}\lambda^2 - \tfrac{3}{5}\lambda R_p + F_0^2 + 2F_2^2$$
$$S_3^3 = \tfrac{2}{35}\lambda^2 - \tfrac{6}{35}\lambda R_p + \tfrac{9}{7}F_2^2$$
$$S_0^4 = -\tfrac{1}{5}\lambda^3 + \tfrac{4}{5}\lambda^2 R_p - 2(F_0^2 + 2F_2^2)\lambda + 4F_1^3$$
$$S_2^4 = -\tfrac{4}{35}\lambda^3 + \tfrac{16}{35}\lambda^2 R_p - (\tfrac{4}{5}F_0^2 + \tfrac{22}{7}F_2^2)\lambda + \tfrac{8}{5}F_1^3 + \tfrac{12}{5}F_3^3$$
$$S_4^4 = -\tfrac{8}{315}\lambda^3 + \tfrac{32}{315}\lambda^2 R_p - \tfrac{8}{7}F_2^2\lambda + \tfrac{16}{9}F_3^3$$

Implementation within a computer code of equations of the form (25) is discussed in I. Noteworthy features of KUBBIC include the incorporation of the two-parameter scattering cross section using the *magic* formula in a form that changes the integration variable from transferred energy (used by all other known transport theory simulation codes) to impact parameter. The numerical solution of the coupled set of integral equations formed is carried out using the residual correction technique proposed by Winterbon (1986). Modifications to KUBBIC were required in order to incorporate the stopping energy E_s. The operator $\mathcal{L}_l$ in the source term of the first-order ODE (equation (30) in I), approximating a correction to the true solution, was modified to include the unit step function and the explicit incorporation of electronic energy loss. Compare equation (3) in I with the new definition given by (25). Note, however, that the treatment of electronic loss for the gas-like model remains the same as before, as demonstrated in the appendix. The maximum impact parameter p_{max} is set in both KUBBIC and MC codes according to scattering within a cylindrical volume $\sigma_n \lambda = 1/N$ with $\lambda = N^{-1/3}$ to give

$$p_{max} = \sqrt{1/\pi N^{2/3}}.$$

(30)

We note parenthetically that, at energies below $\sim 1\,keV$, this value of p_{max} underestimates the elastic energy loss (a similar example can be found in Eckstein (1991) ch 7). In I, KUBBIC employed a different value of p_{max} set to approximately

twice the value given by (30). This value was chosen to facilitate comparison with the KUBBIC code implementing the one-parameter differential nuclear scattering cross section. In the present paper the one-parameter cross section is not considered and, therefore, the overriding objective becomes the consistent comparison between transport theory and MC codes.

7. Results

7.1. Comparison of the gas-like and the liquid models

In figure 2 we compare eight moments of the range distribution for As ions implanted into an amorphous homogeneous Si target of infinite extent using gas-like and liquid models. Comparisons are performed between the revised KUBBIC transport theory code and our parallel processor MC code based on TRIM. The eight moments compared are the mean projected range R_p, vertical straggle σ_z, skewness γ_z, vertical kurtosis β_z, lateral straggle σ_x, lateral kurtosis β_x and the normalized mixed moments $\langle z_{cn} x_n^2 \rangle$ and $\langle z_{cn}^2 x_n^2 \rangle$ (see Ashworth *et al* (1991) for details of the normalization). Comparisons take place over the energy range 1 keV to 1 MeV. The stopping energy E_s is set to 5 eV in both codes. Using KUBBIC, convergence of results must be confirmed in terms of sensitivity to the energy grid and the number of correction iterations. Results using logarithmic energy grids of 20 and 30 points per decade were identical. No significant difference was apparent between results after six and eight iterations (though some slight instability of the moment β_z computed using the liquid model is apparent). Convergence of both gas-like and liquid models is improved using central-moment TE as described in I. However, a delicate trade-off exists between the increased complexity of central-moment TE (i.e. running time per correction iteration) against reduction in the overall running time due to superior convergence. In the current implementations approximately thirty minutes of CPU time on a SUN4/75 is required to perform eight iterations using non-central TE and four iterations using central TE. Moments obtained from the MC code are the result of simulating 10^6 ion trajectories for energies up to 100 keV. The moments obtained at 300 keV are the result of 2.5×10^5 ions and at 1 MeV the result of 10^5 ions. Some details of the MC code have been updated to more closely resemble TRIM-91. For example, the ion is followed using three directional cosines as opposed to the two used in TRIM-85. In addition, the electronic energy loss experienced over the free-flight path is subtracted from the ion energy prior to nuclear scattering using the *magic* formula. The ordered nature of the electronic and nuclear interactions used here is contrasted with TRIM-85 (Ziegler *et al* 1985) where the electronic energy loss and nuclear energy transferred in a collision are computed from the same ion energy and then subtracted simultaneously.

The following comments are made concerning the comparison in figure 2 of gas-like and liquid models. Excellent agreement is obtained between the computer codes, even at very low energies, *when using the same free-flight path models*. Significant deviations occur, however, between the gas-like and liquid models, at energies below ~ 10 keV, when both models are used in the same code. The mean projected ranges and lateral straggles show no significant differences but, for the six remaining moments, divergence becomes apparent at energies below ~ 100 keV and is very noticeable at 10 keV. Below this energy significant deviation can be observed. Figures 3 (1 keV) and 4 (3 keV) compare the projected range profiles of the two
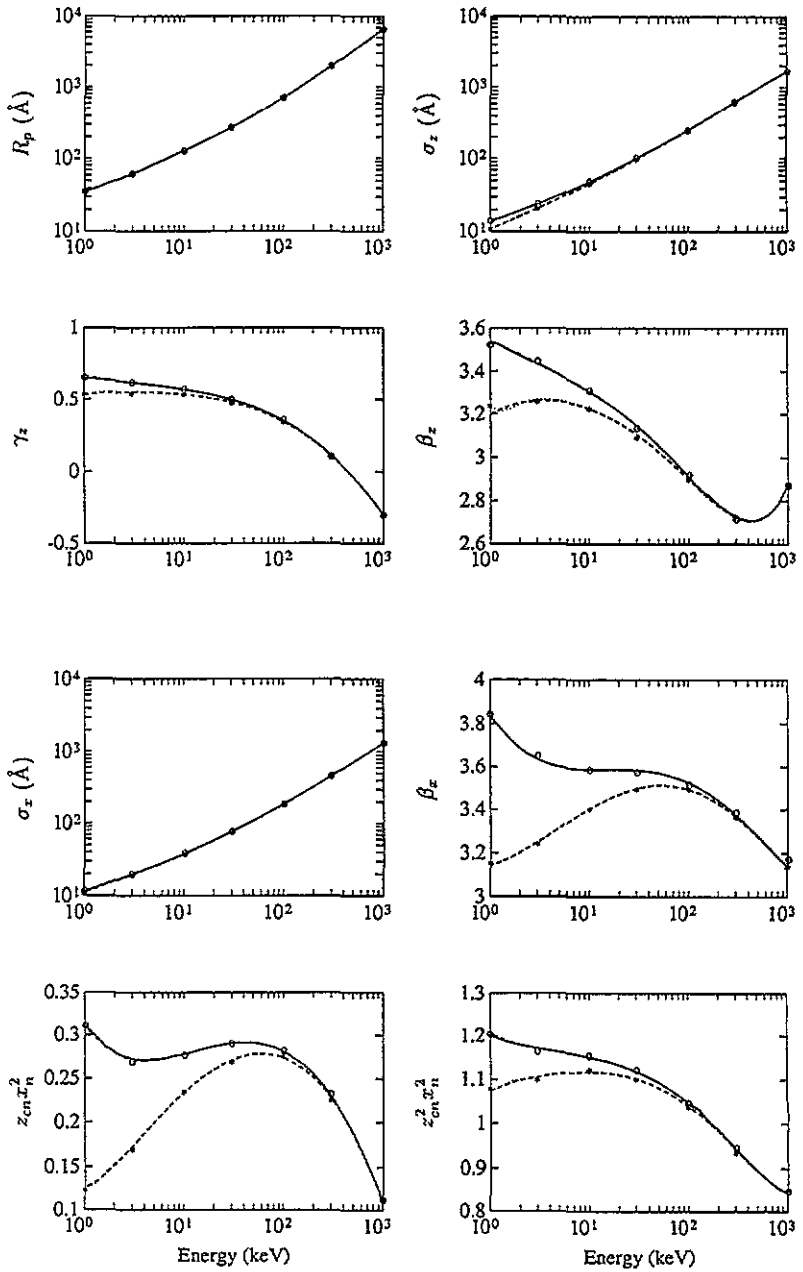
Figure 2. Comparison of moments for As into aSi using gas-like and liquid models with $E_s = 5$ eV: o, MC with the gas-like model; *, MC with the liquid model; ———, KUBBIC with the gas-like model and six iterations; — · —, as before but eight iterations; – – –, KUBBIC with the liquid model and six iterations; ······, as before but ten iterations.

models. In each figure, one profile is generated directly from the MC code and the other is reconstructed from moments generated by KUBBIC. The latter profile is generated using the Pearson function of type I. Full details of various Pearson function types and their applicability to profile construction for various ion–target
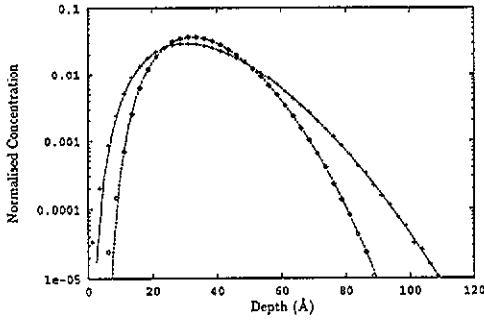
Figure 3. Comparison of projected range profiles for As into aSi at 1 keV using gas-like and liquid models with $E_s = 5$ eV: $\Diamond$, MC with the liquid model; $+$, MC with the gas-like model; $— \cdot —$, Pearson I generated from KUBBIC moments using the gas-like model; $\cdots\cdots$, Pearson I generated from KUBBIC moments using the liquid model.
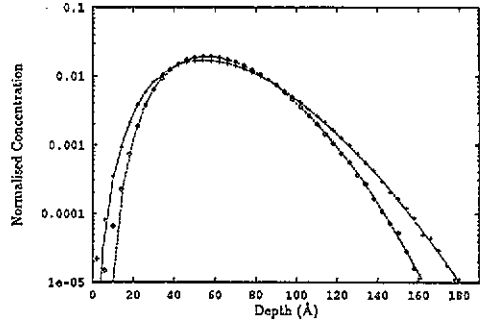
Figure 4. Comparison of projected range profiles for As into aSi at 3 keV using gas-like and liquid models with $E_s = 5$ eV: $\Diamond$, MC with the liquid model; $+$, MC with the gas-like model; $— \cdot —$, Pearson I generated from KUBBIC moments using the gas-like model; $\cdots\cdots$, Pearson I generated from KUBBIC moments using the liquid model.

combinations can be found in Ashworth *et al* (1990) and Bowyer *et al* (1992b). It can be seen from figures 3 and 4 that the differences between the moments in the two models causes the depth profiles to vary significantly.

7.2. Effect of the stopping energy E_s

The new TE includes a minimum energy E_s at which the ion is assumed to stop. In I no such energy was employed. Figure 5 compares KUBBIC runs for both gas-like and liquid models with $E_s = 0$ eV and $E_s = 5$ eV. Considering the results in figure 5, together with the excellent agreement (figure 2) obtained with the MC code (when KUBBIC includes E_s in the transport model), matching the stopping energy is indeed important.

8. Conclusions

A vector transport equation (TE) that incorporates an arbitrary free-flight path distribution and a stopping (or intermediate) energy has been derived. The new TE takes the form of an integral equation in contrast to integro-differential equations derived by prior assumption of the gas-like model. A generator equation has been derived that allows moments up to a given order to be computed. This generator equation has been manipulated into a form in which a solution of the resulting coupled set of integral equations (for Legendre coefficients) can be approached using existing numerical procedures. A generator equation for the liquid model has been derived and a set of eight integral equations, required for the calculation of moments of order up to four, has been presented and implemented in a revised version of the KUBBIC code. A comparison of moments generated using gas-like and liquid models has been performed for the ion As implanted into aSi over the energy range 1 keV to 1 MeV. Excellent agreement between third- and fourth-order moments generated by the KUBBIC code and a MC code based on TRIM has been demonstrated. This was only achieved by a combination of three factors: (i) use of the two-parameter differential
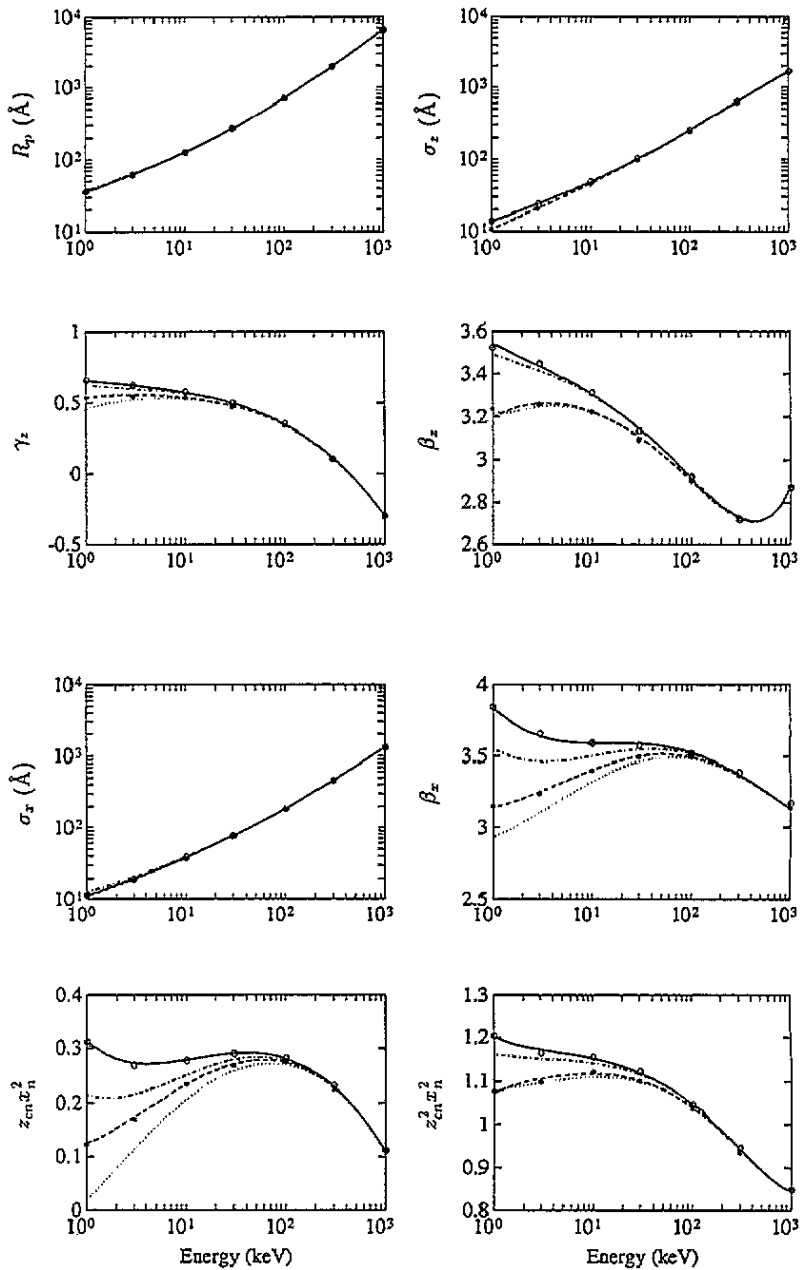
Figure 5. Comparison of moments for As into aSi using minimum energies $E_s = 0\,eV$ and $E_s = 5\,eV$: o, MC with the gas-like model; *, MC with the liquid model; ——, KUBBIC with the gas like model and $E_s = 5\,eV$; — · —, as before with $E_s = 0\,eV$; – – –, KUBBIC with the liquid model and $E_s = 5\,eV$; ······, as before with $E_s = 0\,eV$.

scattering cross section (the default in TRIM); (ii) use of the same free-flight path length model (gas like or liquid) in both the transport theory and the MC codes; and (iii) inclusion of a stopping energy. Significant deviation between gas-like and liquid models is apparent at energies below $\sim 10\,keV$ when both models are used in the

same code.

Appendix

We split the first integral in (11) into two, and write

$$
F(E,\hat{u},E_s,r) = \int_0^{\Delta l} f(l)\left(\int_0^{2\pi}\int_{T_{\min}}^{T_{\max}} F(E',\hat{u}',E_s,r-\hat{u}l)\theta(E'-E_s)\frac{d\tilde{\sigma}_n}{\sigma_n}\frac{d\beta}{2\pi}\right)dl
$$
$$
+ \int_{\Delta l}^{\infty} f(l)\left(\int_0^{2\pi}\int_{T_{\min}}^{T_{\max}} F(E',\hat{u}',E_s,r-\hat{u}l)\theta(E'-E_s)\frac{d\tilde{\sigma}_n}{\sigma_n}\frac{d\beta}{2\pi}\right)dl
$$
$$
+ \int_0^{\infty} f(l)\left(\int_{T_{\min}}^{T_{\max}} \theta(E_s-E')\frac{d\tilde{\sigma}_n}{\sigma_n}\right)\delta(r-\hat{u}l)dl. \tag{A1}
$$

Now, let us consider the probability density

$$
\int_{\Delta l}^{\infty} f(l)\left(\int_0^{2\pi}\int_{T_{\min}}^{T_{\max}} F(E',\hat{u}',E_s,r-\hat{u}l)\theta(E'-E_s)\frac{d\tilde{\sigma}_n}{\sigma_n}\frac{d\beta}{2\pi}\right)dl
$$
$$
+ \int_{\Delta l}^{\infty} f(l)\left(\int_{T_{\min}}^{T_{\max}} \theta(E_s-E')\frac{d\tilde{\sigma}_n}{\sigma_n}\right)\delta(r-\hat{u}l)dl. \tag{A2}
$$

From the derivation in section 2, equation (A2) can be physically interpreted as the probability density that the ion undergoes its first scattering event after travelling a distance $\Delta l < l < \infty$ in the direction $\hat{u}$ and then comes to rest at r. This must equal the probability that the ion travels a distance Δl, *without* being scattered, multiplied by the probability density that the ion comes to rest at r *after* travelling a distance Δl. Since, for a Poisson distribution, $\exp(-\Delta l/\lambda)$ gives the probability the ion will travel a distance Δl without undergoing a nuclear scattering event, the probability density in equation (A2) is therefore equivalent to:

$$
\exp\left(\frac{-\Delta l}{\lambda}\right)F(E-NS_e(E)\Delta l,\hat{u},E_s,r-\hat{u}\Delta l). \tag{A3}
$$

Eliminating the second integral in (A1) by use of equations (A2) and (A3) gives

$$
F(E,\hat{u},E_s,r) = \int_0^{\Delta l} f(l)\left(\int_0^{2\pi}\int_{T_{\min}}^{T_{\max}} F(E',\hat{u}',E_s,r-\hat{u}l)\theta(E'-E_s)\frac{d\tilde{\sigma}_n}{\sigma_n}\frac{d\beta}{2\pi}\right)dl
$$
$$
+ \int_0^{\Delta l} f(l)\left(\int_{T_{\min}}^{T_{\max}} \theta(E_s-E')\frac{d\tilde{\sigma}_n}{\sigma_n}\right)\delta(r-\hat{u}l)dl
$$
$$
+ \exp\left(\frac{-\Delta l}{\lambda}\right)F(E-NS_e(E)\Delta l,\hat{u},E_s,r-\hat{u}\Delta l). \tag{A4}
$$

Expanding the first and third terms in equation (A4) to order Δl gives

$$
F(E,\hat{u},E_s,r) = \frac{\Delta l}{\lambda}\int_0^{2\pi}\int_{T_{\min}}^{T_{\max}} F(E-T_n,\hat{u}',E_s,r)\theta(E-T_n-E_s)\frac{d\tilde{\sigma}_n}{\sigma_n}\frac{d\beta}{2\pi}
$$
$$
+ \int_0^{\Delta l} f(l)\left(\int_{T_{\min}}^{T_{\max}} \theta(E_s-E')\frac{d\tilde{\sigma}_n}{\sigma_n}\right)\delta(r-\hat{u}l)dl
$$
$$
- NS_e(E)\Delta l\frac{\partial F(E,\hat{u},E_s,r)}{\partial E} - \Delta l\hat{u}\cdot\mathrm{grad}_r F(E,\hat{u},E_s,r)
$$
$$
+ F(E,\hat{u},E_s,r) - F(E,\hat{u},E_s,r)\frac{\Delta l}{\lambda} + \mathrm{O}(\Delta l^2). \tag{A5}
$$

Dividing through by Δl and taking the limit $\Delta l \to 0$ gives

$$
\begin{aligned}
- \hat{u} \cdot \mathrm{grad}_r F(E, \hat{u}, E_s, r) = N \int_0^{2\pi} \int_{T_{\min}}^{T_{\max}} & [F(E, \hat{u}, E_s, r) \\
& - F(E - T_n, \hat{u}', E_s, r)\theta(E - T_n - E_s)] \mathrm{d}\tilde{\sigma}_n \frac{\mathrm{d}\beta}{2\pi} \\
& + N S_e(E) \frac{\partial F(E, \hat{u}, E_s, r)}{\partial E} - \delta(r) N \int_{T_{\min}}^{T_{\max}} \theta(E_s - E + T_n)\mathrm{d}\tilde{\sigma}_n
\end{aligned}
$$

(A6)

where we have used

$$
\lim_{\Delta l \to 0} \left(\frac{1}{\Delta l} \int_0^{\Delta l} f(l)g(l)\delta(r - \hat{u}l)\mathrm{d}l \right) = \delta(r)f(0)g(0) = \frac{\delta(r)}{\lambda}g(0)
$$

(A7)

in which $g(l)$ is an arbitrary function of l. Equation (A6) is a vector version of the LSS integro-differential equation, modified to include a stopping (or intermediate) energy. Taking spatial moments and expanding using Legendre polynomials as described in Winterbon *et al* (1970) one obtains (24), a generator equation for the Legendre coefficients $F_l^n(E, E_s)$ for the gas-like model.

References

Ashworth D G, Oven R and Bowyer M D J 1991 *Elec. Lett.* **27** 1402–3
Ashworth D G, Oven R and Mundin B 1990 *J. Phys. D: Appl. Phys.* **23** 870–6
Biersack J P 1982 *Z. Phys.* A **305** 95–101
Bowyer M D J, Ashworth D G and Oven R 1992a *J. Phys. D: Appl. Phys.* **25** 1619–29
—— 1992b *Solid State Electron.* **35** 1151–66
Brice D K 1971 *Radiat. Eff.* **11** 227–40
Eckstein W 1991 *Computer Simulation of Ion–Solid Interactions* (Berlin: Springer)
Lindhard J, Scharff M and Schiøtt H E 1963 *K. Danske Vidensk. Selsk. Mat.-Fys. Meddr.* **33** No 14
Littmark U and Gras-Marti A 1978 *Appl. Phys.* **16** 247–53
Miyagawa Y and Miyagawa S 1983 *J. Appl. Phys.* **54** 7124–31
Robinson M T and Torrens I M 1974 *Phys. Rev.* B **9** 5008–24
Winterbon K B 1986 *Nucl. Instrum. Methods* B **17** 193–202
Winterbon K B, Sigmund P and Saunders J B 1970 *K. Danske Vidensk. Selsk. Mat.-Fys. Meddr.* **87** No 14
Ziegler J F, Biersack J P and Littmark U 1985 *The Stopping and Ranges of Ions in Matter* **1** (ed J F Ziegler) (New York: Pergamon)